

Semianalytic treatment of two-color photoassociation spectroscopy and control of cold atoms

John L. Bohn*

Joint Institute for Laboratory Astrophysics and Quantum Physics Division, National Institute of Standards and Technology, Boulder, Colorado 80309

P. S. Julienne

Atomic Physics Division, National Institute of Standards and Technology, Gaithersburg, Maryland 20899

(Received 6 August 1996)

We present semianalytic expressions for scattering probabilities of cold trapped atoms in the presence of two weak, independently tunable laser fields, both tuned near molecular resonances. We consider two experimental situations. In the first, an Autler-Townes doublet appears and is shown in certain circumstances to exhibit unequal peak heights. In the second, the pair of lasers is employed to produce translationally cold ground-state molecules, in which case our formula suggests the optimal conditions for such production. [S1050-2947(96)50312-4]

PACS number(s): 34.50.Rk, 32.80.Pj, 33.70.Ca

Cold atom traps have recently enabled high-precision photoassociation (PA) spectroscopy of molecular vibrational levels in alkali-metal atom dimers [1–4]. The photoassociation process employs a laser of angular frequency ω_1 to boost a pair of colliding atoms from their initial relative kinetic energy E to a molecular bound level with energy $E_{b1} \approx E + \hbar\omega_1$. Populating this bound level leads generally to spontaneous emission or other trap loss processes, whose rate versus laser detuning thus maps out the spectrum of molecular vibrations. The observed line shapes represent thermal averages over the distribution of trapped atom energies, which can be comparable to, or smaller than, natural linewidths at the mK temperatures in magneto-optical traps (MOTs). In addition, extremely low collision energies produce a suppression of scattering rates near threshold in accordance with the Wigner threshold law. These considerations imply that the bound level's energy is not given simply by the energy of the PA laser which produces the maximum signal, but must be culled from a detailed treatment of the thermally averaged line shape. Such line shapes have been presented, and agree well with the shapes measured in high-resolution PA spectroscopy [5].

Recently, steps have been taken to extend PA spectroscopy to the two-color regime, employing a second laser of angular frequency ω_2 to drive the dimer from bound level E_{b1} to a second bound level E_{b2} . A two-color experiment has successfully determined the triplet s -wave scattering length of ${}^7\text{Li}$ [6], and similar experiments are underway in rubidium [7]. This type of experiment, depicted schematically in Fig. 1(a), probes the high-lying bound states of the ${}^3\Sigma_u^+$ ground-state potential ($\equiv g$) starting with spin polarized alkali-metal atoms and passing through an intermediate bound level of an excited potential (the $b\ {}^3\Sigma_g^+$ potential in Ref. [6]). Laser 1 is detuned by an amount $\Delta_1 \equiv E_{b1} - \hbar\omega_1$ relative to the excited level E_{b1} , while laser 2 is detuned by $\Delta_2 \equiv E_{b2} - \hbar(\omega_1 - \omega_2)$ from E_{b2} . The experiment then con-

sists of varying the detunings and intensities of both lasers, and monitoring fluorescence from the decay of bound level E_{b1} . As in the one-color case, understanding the resulting line shapes will prove essential in ferreting out detailed spectroscopic information.

Beyond spectroscopy, application of a second laser also affords opportunities for manipulating slow atoms. A recent proposal suggests a means of producing translationally cold ground-state molecules by the scheme depicted in Fig. 1(b) [8]. Here the second bound level lies *above* the first, in a molecular Rydberg potential (${}^1\Pi_u$ in the sodium example of Ref. [8]), which is expected to decay spontaneously into several of the lowest-lying vibrational levels of the ${}^1\Sigma_g$ ground-state potential. In this case the second laser's detuning is given by $\Delta_2 \equiv E_{b2} - \hbar(\omega_1 + \omega_2)$. Understanding the production of cold molecules in this scheme requires a simple interpretive framework. Accordingly, we show in this paper how semianalytic line-shape formulas can serve both as interpretive tools and as guides for two-color manipulation of cold atoms.

In both experiments an incident pair of colliding atoms is transformed by a light-assisted collision process into one or more reaction products p , which we will consider as continuum exit channels in the sense of scattering theory. We therefore model PA spectroscopy by computing rate coefficients for the production of p :

$$K_p(T, \Delta_1, \Delta_2, I_1, I_2) = \left\langle \frac{\pi v}{k^2} \sum_{l=0}^{\infty} (2l+1) |S_{pg}(E, l, \Delta_1, \Delta_2, I_1, I_2)|^2 \right\rangle. \quad (1)$$

Here I_i refers to laser i 's intensity, while $E = \hbar^2 k^2 / 2\mu = \mu v^2 / 2$, v is the relative velocity and μ the reduced mass of the colliding pair. S_{pg} represents the scattering matrix element for producing the product p from the initial ground state g . The sum in Eq. (1) is taken over all partial waves l , and is finally averaged over the distribution of velocities in the trap, implied by the angular brackets. This distribution has typically the Maxwell-Boltzmann form

*Electronic address: bohn@jilac.colorado.edu

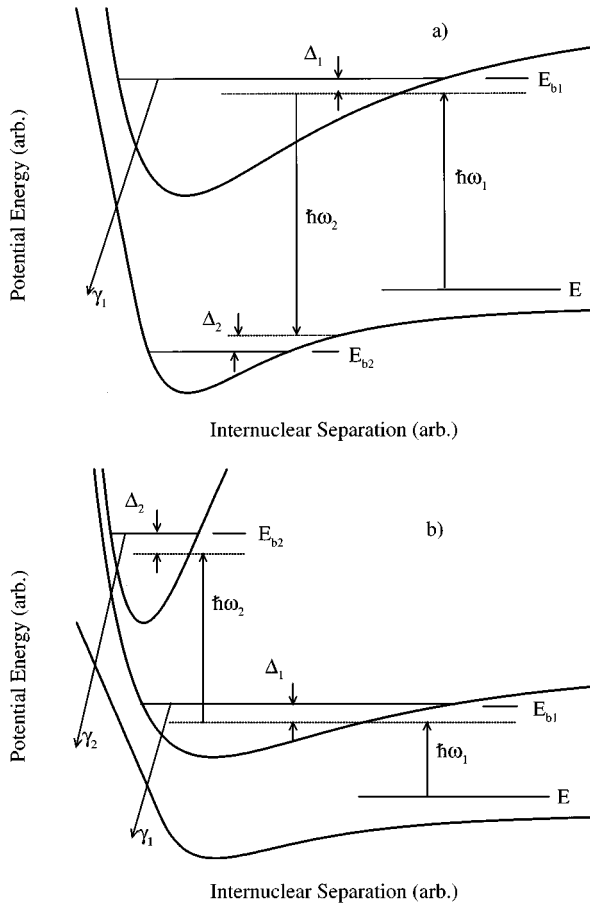


FIG. 1. Schematic alkali-metal atom potential curves for the processes considered, along with the bound levels and the laser frequencies that move between them. In (a), only level b_1 can decay by spontaneous emission, whereas in (b), both bound levels may decay. We consider only isolated resonances, in particular ignoring hyperfine structure.

for a MOT, but will take other forms at temperatures near or below the phase transition to Bose-Einstein condensation.

Reference [5] stressed that for sufficiently low laser intensities, the *one-color* scattering probability takes the pseudo-Lorentzian form

$$|S_{1g}(E, l, \Delta_1, I_1)|^2 = \gamma_1 \gamma_s(E, l, I_1) / [(E - \Delta_1)^2 + (\gamma/2)^2]. \quad (2)$$

Here the total width γ is the sum of two partial widths: $\gamma_s(E, l, I_1)$, representing stimulated emission back to the ground state, and γ_1 , representing the decay width for spontaneous emission from level b_1 . For weak laser light, Fermi's golden rule determines the stimulated width by $\gamma_s(E, l, I_1) \approx 2\pi V_1^2 |(b_1|E, l)|^2$, involving the Franck-Condon overlap between the energy-normalized incident wave $|E, l\rangle$ and the bound-state wave function $|b_1\rangle$. The action of laser 1 is given by the radiative coupling matrix element $V_1(R) = (2\pi I_1/c)^{1/2} d_1(R)$, proportional to a molecular dipole matrix element $d_1(R)$, and typically expressed as a Rabi frequency $\Omega_1 = V_1/\hbar$. Generally d_1 depends weakly on the internuclear distance R for high-lying bound levels; we will assume that d_1 is constant in the following. Note that the Wigner threshold law is built into the squared-Franck-Condon factor, which vanishes as $E^{1/2}$ near threshold for

S -wave scattering. The expression (2) has been shown previously to agree with full close-coupling calculations in the limit of weak laser light [5].

We remark here that the semianalytic expression (2) already tells us something about controlling cold collisions. First, the maximum diversion of flux into product p_1 is, of course, achieved at the resonant energy $E = \Delta_1$, which is at the experimenter's disposal. Moreover, the *total yield* of the product attains its maximum value, $|S_{1g}|^2 = 1$, precisely when $\gamma_s = \gamma_1$; that is, when the rate γ_s/\hbar at which incident flux flows into the resonant channel exactly matches the rate γ_1/\hbar at which the product is produced. This circumstance enables the experimenter, in principle, to shut off flux back into the incident channel altogether.

We begin our discussion of the two-color case by presenting the scattering probability for producing product p_1 from the decay of bound level b_1 in Fig. 1(a),

$$|S_{1g}|^2 = \frac{(E - \Delta_2)^2 \gamma_1 \gamma_s}{[(E - \Delta_+)(E - \Delta_-)]^2 + (\gamma/2)^2 (E - \Delta_2)^2}. \quad (3)$$

The second laser thus splits a single scattering resonance into a pair of peaks located near the energies

$$\Delta_{\pm} = \frac{1}{2}(\Delta_1 + \Delta_2) \pm \frac{1}{2}\sqrt{(\Delta_1 - \Delta_2)^2 + 4h^2\Omega_{12}^2}. \quad (4)$$

The widths γ_1 and γ_s are as defined above, while $h\Omega_{12} = V_2 \langle b_1 | b_2 \rangle$ represents the molecular Rabi coupling, proportional to the radiative coupling V_2 (defined analogously with V_1) and to the bound-bound Franck-Condon factor. (Our convention differs from that of Ref [12], so that $2\Omega_{12}$ represents the Rabi frequency for transferring amplitude between the two bound states.) The energy shifts (4) will also be accompanied by additional shifts, as is generally the case for bound levels embedded in a continuum [9]. These shifts become more prominent at higher laser intensities, and do not affect our conclusions here. Notice that when the second laser is switched off, setting $\Omega_{12} = 0$, we recover the one-color scattering profile (2).

We have derived the two-color formula (3) in the context of the generalized multichannel quantum defect theory (GMQDT) [10], which presents detailed scattering resonance shapes given a modest amount of input information on a scattering process. This input consists of a short-range "reaction matrix," which usually emerges from a full solution of the relevant coupled Schrödinger equations, but in the present context of weak laser intensity is given perturbatively in terms of Franck-Condon factors. A full account of the derivation of Eq. (4) will be given separately [11], along with the accurate close-coupling calculations that exhibit power broadening and energy shifts at higher laser intensities.

The character of the pair of peaks is conveniently parameterized by a mock angle $\chi \equiv \tan^{-1}[2h\Omega_{12}/(\Delta_1 - \Delta_2)]$, representing the strength of the bound-bound Rabi coupling, normalized by the *relative detuning*. A value of χ near $\pi/2$ means that $\Delta_1 \approx \Delta_2$, i.e., that laser 2 is nearly resonant with the energy difference $E_{b1} - E_{b2}$, yielding a scattering profile like that shown in Fig. 2(a). The dashed line represents the one-color scattering profile for a detuning $\Delta_1/\hbar = 10$ MHz of

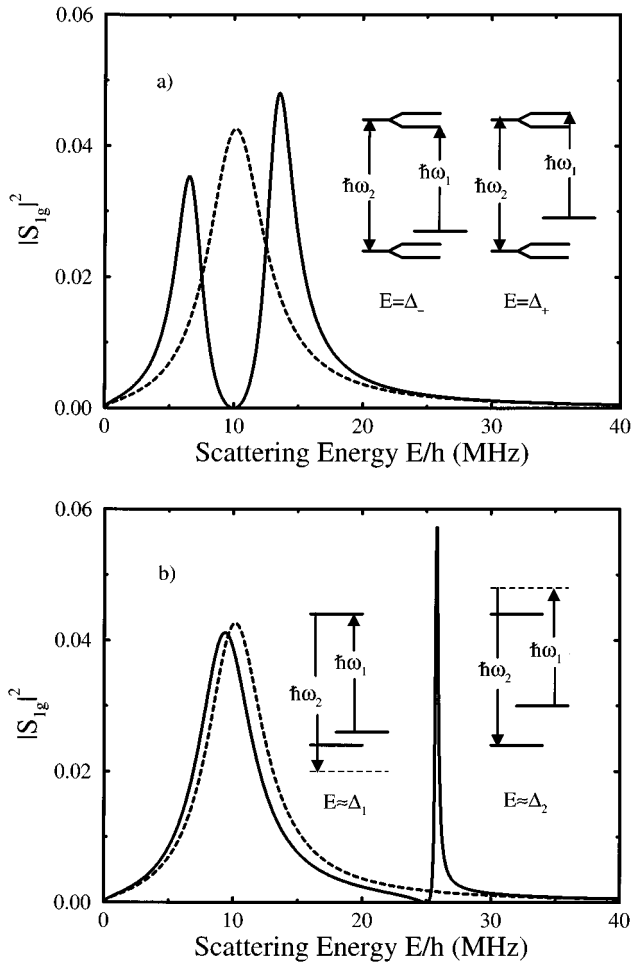


FIG. 2. S -wave scattering profiles $|S_{1g}(E)|^2$ for cold atom scattering in the presence of laser 1 alone (dashed lines) and both lasers (solid lines). In this example, b_1 stands for the $v=64$ vibrational level of the $b \ ^3\Sigma_g^+$ potential, and b_2 for the $v=10$ vibrational level of the $^3\Sigma_u^+$ + ground-state potential, following Ref. [6]. In both (a) and (b), $\Omega_1=100$ MHz, $\Delta_1/h=10$ MHz, and $\Omega_{12}=4.0$ MHz. (a) shows the strongly field-dressed case, $\Delta_2/h=10$ MHz ($\chi=\pi/2$), in which the one-color peak splits nearly in half. (b) shows a less strongly field-dressed case, $\Delta_2/h=25$ MHz ($\chi\approx-0.5$). The inset energy-level diagrams illustrate different ways of viewing the pair of scattering resonances in the two cases.

laser 1, thus exhibiting a scattering peak at $E/h=10$ MHz. The solid line gives the scattering profile in the presence of both lasers, with laser 2's detuning set also to $\Delta_2/h=10$ MHz. In this case the strong coupling between bound levels produces a Rabi splitting, indicated schematically in the level diagrams of Fig. 2(a). For a fixed ‘‘probe’’ laser frequency ω_1 , the colliding atoms see resonances at two distinct incident energies $E=\Delta_{\pm}$, indicated by the two insets. In the field-dressed atom picture these two resonances represent roughly equal linear combinations of the two bound levels, yielding peaks of roughly equal width. Note, however, that the peak closer to threshold is smaller, a by-product of the Wigner threshold law.

Figure 2(b) shows instead an alternative case where $\chi\approx-0.5$, representing a more perturbative regime in which the one-color scattering profile is only slightly altered by switching on laser 2. In this figure $\Delta_1/h=10$ MHz as before,

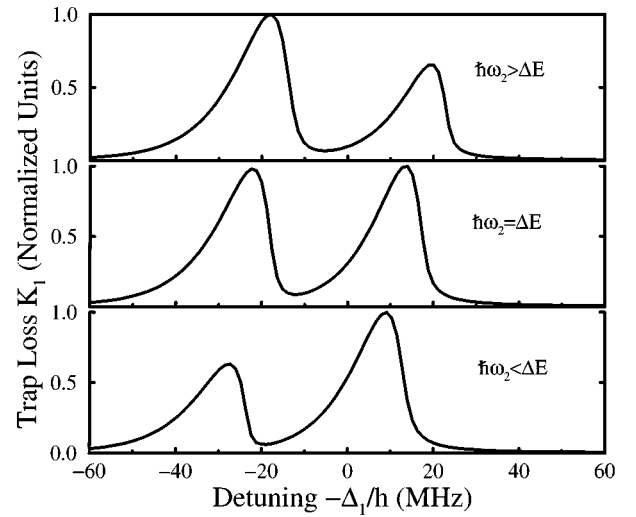


FIG. 3. Thermally averaged line shapes for a trap temperature of 1 mK, showing the Autler-Townes doublet. Here $\Omega_1=100$ MHz and $\Omega_{12}=20$ MHz. In each case $\hbar\omega_2$ is fixed near the energy difference $\Delta E=E_{b_1}-E_{b_2}$ between the bound levels, and Δ_1 is scanned. In the top (bottom) panel laser 2 is blue (red) detuned by 10 MHz, while in the middle panel, laser 2 is resonant with ΔE .

but laser 2 has been detuned to $\Delta_2/h=25$ MHz. In this far-detuned case, the field-dressed picture is no longer the appropriate frame in which to view the scattering. Rather, the broad peak lies at a scattering energy E that can be boosted directly to level E_{b_1} by $\hbar\omega_1$, as shown in the left-hand inset. The narrower peak, requiring a higher scattering energy in this example, is generated when the relative laser energy $\hbar(\omega_1-\omega_2)$ hits level E_{b_2} , as shown in the right-hand inset; however, this two-photon process can proceed only by a virtual excitation in the first step, rendering this peak narrow. In fact, from Eq. (3) it follows that the width of the narrow peak scales as $\tan^2\chi$ in this limit.

The scattering peaks are separated by a ‘‘dark spot,’’ i.e., a zero of scattering probability, when $E=\Delta_2$, arising from destructive interference between the two scattering paths $g\rightarrow b_1\rightarrow p_1$ and $g\rightarrow b_1\rightarrow b_2\rightarrow b_1\rightarrow p_1$. This dark spot represents a form of two-color control of the scattering, enabling the experimenter to shut off production of p_1 . Alternatively, tuning to either of the resonances at Δ_{\pm} and meeting the rate matching condition $\gamma_s=\gamma_1$ will shut off the output of channel g , just as in the one-color case.

For sufficiently large splitting the twin-peaked structure will survive thermal averaging and appear as an Autler-Townes doublet [12]. To observe the doublet, laser 2 is fixed on an energy at or near the energy difference $\Delta E=E_{b_1}-E_{b_2}$ between the two bound levels, and laser 1 is scanned to search for the pair of peaks. Detuning laser 1 for fixed $\hbar\omega_2$ passes first one scattering peak, then the other, through the thermal distribution of trapped atoms, yielding two peaks in the trap loss spectrum. Three such spectra are shown in Fig. 3, which assumes a trap temperature of 1 mK. The relative sizes of the peaks depend on the parameter χ , and are nearly equal when $\chi\approx\pi/2$, as in the center panel. Otherwise laser 2's detuning determines which peak is larger. If laser 2 is tuned *blue* of the bound-bound transition ($\hbar\omega_2>\Delta E$, which implies $\Delta_2>\Delta_1$) the scattering probabil-

ity exhibits a broader peak at lower energy and a narrower peak at higher energy, as in the example shown in Fig. 2(b). The larger Autler-Townes peak therefore lies at redder detuning of laser 1, as shown in the top panel of Fig. 3. For *red* detuning of laser 2, the reverse is true, as shown in the bottom panel. Asymmetries of the Autler-Townes peak heights have in fact been observed by Abraham [13]. Symmetry of

the peak heights may serve as a diagnostic tool for deciding when laser 2 is on resonance between the two bound levels.

We turn now to the manipulation experiment of Fig. 1(b) [8]. Now there are two products, p_1 and p_2 , representing spontaneous emissions from bound levels b_1 and b_2 . The product of interest for producing ground-state molecules is p_2 , whose scattering probability is given by

$$|S_{2g}|^2 = \frac{\gamma_2 \gamma_s \Omega_{12}^2}{[(E - \Delta_+)(E - \Delta_-) - \gamma_2(\gamma)/4]^2 + [\gamma_2(E - \Delta_1)/2 + \gamma(E - \Delta_2)/2]^2}, \quad (5)$$

where $\gamma = \gamma_s + \gamma_1$, as in the one-color case. The resonance positions Δ_{\pm} here experience additional shifts governed by the term $\gamma_2\gamma/4$, representing the influence of the additional continuum p_2 . The scattering probabilities for producing product p_1 and for elastic scattering are proportional to

$$|S_{1g}|^2 \propto [(E - \Delta_2)^2 + \gamma_2^2/4] \gamma_1 \gamma_s, \quad (6)$$

and

$$|S_{gg}|^2 \propto [(E - \Delta_+)(E - \Delta_-) - \gamma_2(\gamma_1 - \gamma_s)/4]^2 + [\gamma_2(E - \Delta_1)/2 + (\gamma_1 - \gamma_2)(E - \Delta_2)/2]^2, \quad (7)$$

respectively, and have the same resonance denominator as in Eq. (5). Whereas in the previous case the scattering probability vanished when $E = \Delta_2$, here the dark spot is merely ‘‘gray.’’ In this case flux is lost from level b_2 , so the interference between the paths $g \rightarrow b_1 \rightarrow p_1$ and $g \rightarrow b_1 \rightarrow b_2 \rightarrow b_1 \rightarrow p_1$ remains incomplete, and $|S_{1g}|^2$ has a minimum rather than a zero. This minimum actually vanishes as the loss rate from b_2 diminishes and the interference becomes more complete. Similarly, emission from b_2 never experiences a dark spot.

To direct the laser-assisted scattering process toward production of p_2 requires simultaneously minimizing the other scattering processes $|S_{1g}|^2$ and $|S_{gg}|^2$ at a suitable scattering energy E_{mol} , which should lie within the thermal distribution of atoms. This requirement is met by the following conditions on the lasers’ characteristics:

$$\Delta_1 = \Delta_2 = E_{\text{mol}}, \quad \gamma_s = \gamma_1 + (2h\Omega_{12}/\gamma_2)^2. \quad (8)$$

The first condition requires that both lasers be exactly on resonance with the unperturbed bound levels. The second condition represents a matching of rates, analogous to the condition $\gamma_s = \gamma_1$ required to set $|S_{1g}|^2 = 1$ above. Again the rate γ_s/\hbar for diverting incident flux into the resonant channels must equal the total rate at which these channels decay. This total rate is a sum of b_1 ’s decay rate γ_1/\hbar , plus a *modified* rate $(2\Omega_{12}/\gamma_2)^2 \gamma_2/\hbar$ for the decay of b_2 . This modification implies that, if the Rabi frequency $2\Omega_{12}$ is less than the decay rate γ_2/\hbar , the decay process has to wait for b_2 to be populated before it can decay; the effective rate is thus smaller. Vice versa, if the Rabi frequency is much larger than the lifetime, level b_2 is continually replenished, enhancing the observed rate.

If these conditions are met, the resonant scattering probability for producing p_2 becomes

$$|S_{2g}(E = E_{\text{mol}})|^2 = 4h^2\Omega_{12}^2/(4h^2\Omega_{12}^2 + \gamma_1\gamma_2), \quad (9)$$

which can be made arbitrarily close to unity by increasing the power of laser 2 [by Eq. (8) this requires also increasing the power of laser one]. Increased laser power will of course bring about energy shifts and saturation effects [11], but we expect the present results to provide useful guidelines for control parameters, as well as for interpretation of the scattering processes involved.

We gratefully acknowledge conversations with W. Clark, B. Esry, C. H. Greene, G. Miecznik, and C. Williams. J.L.B. also acknowledges financial support from the NRC.

-
- [1] H. R. Thorsheim, J. Weiner, and P. S. Julienne, *Phys. Rev. Lett.* **58**, 2420 (1987).
 [2] L. P. Ratliff, M. E. Wagshul, P. D. Lett, S. L. Rolston, and W. D. Phillips, *J. Chem. Phys.* **101**, 2638 (1994).
 [3] K. M. Jones, P. S. Julienne, P. D. Lett, W. D. Phillips, E. Tiesinga, and C. J. Williams, *Europhys. Lett.* **35**, 85 (1996).
 [4] J. D. Miller, R. A. Cline, and D. J. Heinzen, *Phys. Rev. Lett.* **71**, 2204 (1993); R. A. Cline, J. D. Miller, and D. J. Heinzen, *ibid.* **73**, 632 (1994).
 [5] R. Napolitano, J. Weiner, C. J. Williams, and P. S. Julienne, *Phys. Rev. Lett.* **73**, 1352 (1994).
 [6] E. R. I. Abraham, W. I. McAlexander, C. A. Sackett, and R. G. Hulet, *Phys. Rev. Lett.* **74**, 1315 (1995).
 [7] D. Heinzen (private communication).
 [8] Y. B. Band and P. S. Julienne, *Phys. Rev. A* **51**, R4317 (1995).
 [9] U. Fano, *Phys. Rev.* **124**, 1866 (1961).
 [10] F. H. Mies, *J. Chem. Phys.* **80**, 2514 (1984); C. H. Greene, U. Fano, and G. Strinati, *Phys. Rev. A* **19**, 1485 (1979); C. H. Greene, A. R. P. Rau, and U. Fano, *ibid.* **26**, 2441 (1982).
 [11] J. L. Bohn and P. S. Julienne (unpublished).
 [12] C. Cohen-Tannoudji, I. Dupont-Roc, and G. Grynberg, *Atom-Photon Interactions* (John Wiley and Sons, New York, 1992).
 [13] E. R. I. Abraham, Ph.D. thesis, Rice University, 1996 (unpublished).